



# NMR side-chain assignments of the Crimean-Congo haemorrhagic fever virus glycoprotein n cytosolic domain

Louis Brigandat<sup>#1</sup>, Maëlys Laux<sup>#1</sup>, Caroline Marteau<sup>1</sup>, Laura Cole<sup>1</sup>, Anja Böckmann<sup>1</sup>, Lauriane Lecoq<sup>1</sup>, Marie-Laure Fogeron<sup>1</sup>, Morgane Callon<sup>1</sup>

5

<sup>1</sup>MMSB Lyon, UMR5086 CNRS /Lyon University, 7, passage du Vercors, 69367 Lyon Cedex 07, France

<sup>#</sup>These authors contributed equally to this work

*Correspondence to:* Morgane Callon (morgane.callon@ibcp.fr)

## Abstract

10 We assigned the side-chain resonances of the Crimean-Congo haemorrhagic fever virus (CCHFV) glycoprotein n (Gn) cytosolic (cyto) domain to complete the backbone resonances previously published by Estrada et al. (2011). The process was accelerated by three major factors: first, sample preparation using cell-free protein synthesis (CFPS) was completed in less than 2 days and allowed correct zinc finger formation by adding zinc ions to the reaction. Second, remote access to NMR platforms with standardized pulse sequences allowed data acquisition in 18 days. Third, data analysis using the online platform  
15 NMRtist allowed sequential resonance assignments to be made in a day, verified and finalized in less than a week. Our work thus provides an example of how NMR assignments, including side chains, of small and well-behaved proteins can be approached in a rapid routine, at protein concentrations of 150  $\mu$ M.

## 1. Introduction

The Bunyavirales order is a large group of serologically related, often tripartite, negative-sense RNA viruses. Crimean-Congo  
20 haemorrhagic fever virus (CCHFV), a member of the order, is considered one of the most deadly viruses, with a mortality rate of up to 40 % (Ye et al., 2022; Hawman and Feldmann, 2023). CCHFV poses a serious threat to both human and animal health, and is currently spreading to non-endemic areas as their vectors expand their range with global warming. Indeed, the Hyalomma ticks that transmit CCHFV are already present in Europe (Bonnet et al., 2022), and the virus has caused human fatalities in Spain (Lorenzo Juanes et al., 2023); it also has been recently (2023) detected for the first time in southern France.  
25 The three genomic segments of most Bunyavirales can be divided into the small (S), the medium (M), and the large (L) segments. Bunyavirales often share a similar protein composition, consisting of the nucleocapsid (NP) protein, which forms the ribonucleoprotein (RNP) complex with the viral genomes, the two envelope proteins Gn and Gc, and the RNA-dependent RNA polymerase (RdRp). Structural information is abundant for NP (*e.g.* (Sun et al., 2018; Arragain et al., 2019)) and also for RdRp (*e.g.* (Arragain et al., 2019, 2020, 2022)). The Gn and Gc envelope glycoproteins are inserted into the endoplasmic



30 reticulum (ER) during translation and eventually localize to the surface of the viral particle, forming the trimeric spikes that  
characterize mature particles. Gn and Gc have a large ectodomain, a transmembrane anchor and a small cytosolic domain  
(Hulswit et al., 2021). In particular, the Gc ectodomain has been extensively studied (Zhu et al., 2017; Guardado-Calvo and  
Rey, 2017; Bignon et al., 2019; Mishra et al., 2022). In contrast, its transmembrane and cytosolic domains (Gc<sup>TMcyto</sup>) have not  
yet been structurally characterized. For some viruses, information is available for the Gn ectodomain (Hastie et al., 2017;  
35 Hulswit et al., 2021). The Gn ectodomain interacts with the one of Gc and undergoes extensive structural changes during  
maturation (Halldorsson et al., 2018). Several structures exist for the isolated cytosolic domain of Gn (Gn<sup>cyto</sup>), typically from  
Hanta, CCHF and Junin viruses (Estrada et al., 2009; Estrada and De Guzman, 2011). This domain contains a double  $\beta\alpha$  zinc  
finger (ZF) motif that could play a matrix protein role in viral particle assembly (Strandin et al., 2013), as does the Lassa virus  
Z protein, which alone is sufficient for the release of virus-like particles (Strecker et al., 2003).

40 The sequential NMR resonance assignments of CCHFV Gn<sup>cyto</sup> have been reported in the literature, and were deposited  
in the BMRB under the accession number 17383 (Estrada and De Guzman, 2011). Amide proton and <sup>13</sup>C/<sup>15</sup>N backbone  
resonances are presented there, alongside with C $\beta$  assignments. However, other <sup>13</sup>C side chain resonances as well as protons  
remained unassigned. Because of our interest in eventually comparing the isolated domain with the membrane-bound form  
and its likely multimeric states, which we will address using proton-detected magic-angle-spinning NMR, we now report here  
45 the <sup>1</sup>H, <sup>13</sup>C side-chain resonance assignments, as well as the cell-free sample preparation procedures we used to efficiently  
prepare the protein domain.

## 2. Materials and Methods

### 2.1 Wheat-germ cell-free protein synthesis (WG-CFPS)

For WG-CFPS, the sequence corresponding to the cytosolic domain of Gn (residues 733-799) was cloned into the pEU-E01-  
50 MCS vector (CellFree Sciences, Japan) with a Strep-tag fused at its C-terminus. The plasmid was then amplified in DH5 $\alpha$  cells  
and purified using a NucleoBond Xtra Maxi kit (Macherey-Nagel, France). Further purification was performed by phenol-  
chloroform extraction to achieve the required level of plasmid purity. mRNA transcription was performed using 100 ng/ $\mu$ l  
plasmid, 2.5 mM NTP mix (Promega, France), 1U/ $\mu$ l RNase inhibitor (CellFree Sciences, Japan) and 1U/ $\mu$ l SP6 RNA  
polymerase (CellFree Sciences, Japan) in transcription buffer containing 80 mM Hepes-KOH pH 7.6, 16 mM magnesium  
55 acetate, 10 mM DTT and 2 mM spermidine (CellFree Sciences, Japan). The solution was incubated at 37 °C for 6 h, and the  
mRNA produced was used directly for translation. Cell-free synthesis was performed with uncoupled transcription and  
translation. All steps followed the protocol of Takai and colleagues (Fogeron et al., 2017; Takai et al., 2010). Translation  
reactions were performed using the bilayer method for 16 h at 22°C. Uniform <sup>2</sup>H-<sup>13</sup>C-<sup>15</sup>N or <sup>13</sup>C-<sup>15</sup>N labeled amino acids were  
used for sample preparation. The sample was purified by affinity chromatography using a 1-ml *Strep-Tactin*® Superflow®  
60 gravity flow column (IBA Lifesciences). The protein was eluted in 50 mM phosphate buffer pH 6.5, 50 mM NaCl and 2.5 mM  
desthiobiotin, and concentrated using a 3 kDa Amicon Ultra filter to 109  $\mu$ M (<sup>2</sup>H-<sup>13</sup>C-<sup>15</sup>N sample) and 150  $\mu$ M (<sup>13</sup>C-<sup>15</sup>N



sample) as measured using a NanoDrop, and 1x EDTA-free protease inhibitor was added to the final sample to avoid protein degradation. Zinc sulfate was added to each buffer in the manufacturing process at a concentration of 100  $\mu\text{M}$ .

## 2.2 NMR spectroscopy

65 NMR spectra were acquired at 298 K on Bruker Avance III 600 MHz (3D spectra for backbone assignments) and 950 MHz (3D spectra for side-chain assignments) spectrometers equipped with a cryoprobe. Backbone  $^1\text{H}$ ,  $^{15}\text{N}$  and  $^{13}\text{C}$  resonance assignments were performed using standard NMR experiments set up via the NMRlib tool (Favier and Brutscher 2019) in TopSpin 4.0.8 (Bruker Topspin). Specifically,  $^{15}\text{N}$ -HSQC, HNCA, HNCO, HNcaCO, and HNCACB were recorded for backbone assignment, and  $^{13}\text{C}$ -HSQC, HccoNH-TOCSY, hCCH-TOCSY and HCcH-TOCSY were recorded for sidechain  
70 assignment (an  $^{15}\text{N}$ -HSQC was recorded equally on the protonated sample to transfer  $^1\text{H}$ - $^{15}\text{N}$  chemical shifts to the protonated protein). DSS was used for  $^1\text{H}$  chemical shift referencing. All spectra were processed using TopSpin 4.0.8 (Bruker Biospin) and spectra analysis and backbone assignment were performed using CcpNmr v3 (Vranken et al. 2005; Stevens et al. 2011). Sidechain assignment was performed using NMRtist (<https://nmrtist.org/>) and manually validated using CcpNmr v3.

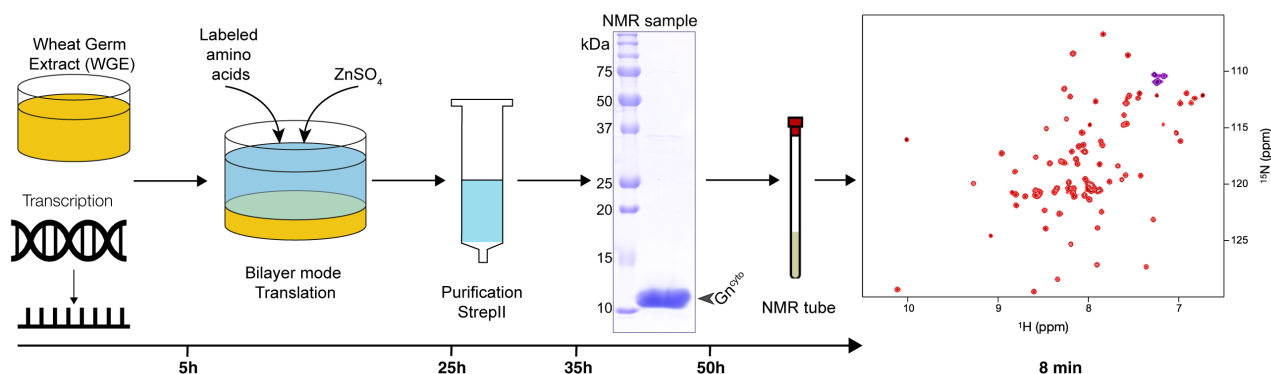
## 3. Results

### 75 3.1 Efficient NMR sample preparation using wheat-germ cell-free protein synthesis

Wheat-germ cell-free protein synthesis (CFPS) was used to prepare the NMR sample. This allowed rapid and efficient preparation of the protein domain, and provided sufficient amounts for NMR. Since it has been shown that supplementation with zinc ions significantly increases the solubility and stability of zinc-binding proteins (Matsuda et al., 2006; Jirasko et al., 2020), we investigated whether the addition of  $\text{ZnSO}_4$  stabilizes the fold of the Gn zinc finger (ZF) domain by using circular  
80 dichroism (CD) and the addition of EDTA to determine under which conditions the folded protein is obtained (Fig. S1). The CD spectra clearly show that the zinc-finger formation is EDTA-dependent and reversible, and that the fold appears more stable when  $\text{ZnSO}_4$  is added. This shows that folded  $\text{Gn}^{\text{cyto}}$  can be obtained in CFPS by simply adding  $\text{ZnSO}_4$  to the reaction. Fig. 1 summarizes the sample preparation workflow, the pure protein preparation used to record the spectra, and the HSQC fingerprint spectrum obtained.



85



90

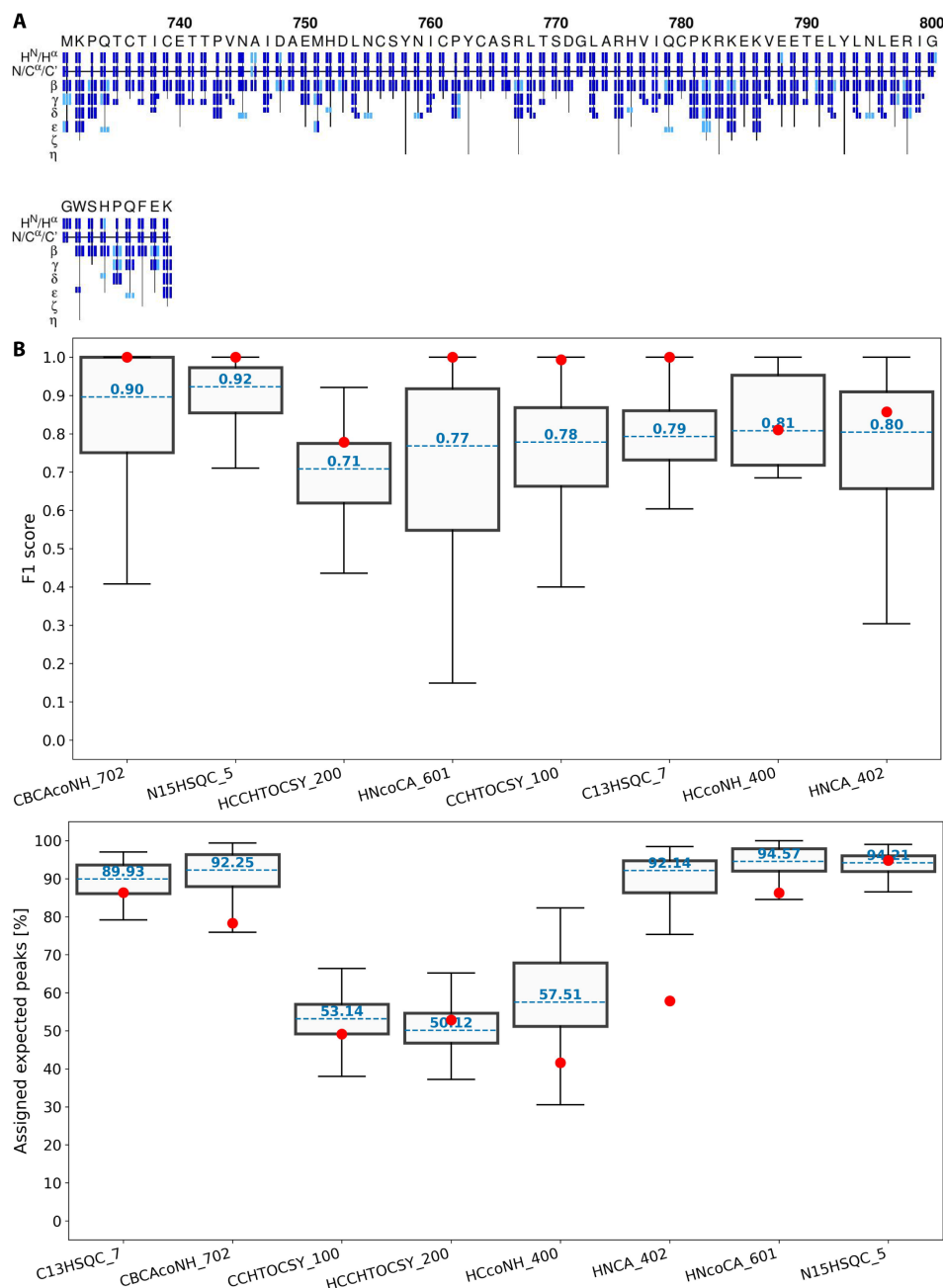
**Figure 1: Workflow for sample preparation.** Wheat germ extract and mRNA encoding the protein are used in a bilayer cell-free reaction. Addition of protonated or deuterated  $^{13}\text{C}/^{15}\text{N}$  labeled amino acids allowed synthesis of labeled protein. Zinc sulphate was added to the reaction to ensure correct zinc finger formation. After a single-step purification using the C-terminal Strep-II tag with concomitant buffer exchange, the protein showed high purity and was filled into the NMR tube. The entire sample preparation took approximately 2 days. The SOFAST HN HSQC spectrum was acquired in 8 minutes.

### 3.2 NMR backbone assignments

The backbone assignments for the  $\text{H}^{\text{N}}$ ,  $\text{N}^{\text{H}}$ ,  $\text{C}\alpha$ ,  $\text{C}\beta$ , and  $\text{H}\alpha$  of  $\text{Gn}^{\text{cyto}}$  have been reported in the literature (Estrada and De Guzman, 2011). In a first step, we analyzed the protein sample to confirm that the zinc finger fold was correctly obtained in the cell-free sample by comparing the NMR chemical shifts here obtained to previous data. To do this, we prepared a deuterated sample, and recorded fingerprint and backbone correlation spectra, including  $^1\text{H}$ - $^{15}\text{N}$  HSCQ, HNCA, HNCO, HNcoCA, and HNcoCACB. The HNCO was used to add the carbonyl assignments not previously determined. The HSQC spectra looked quite different at a first sight (Fig. S2), but this was mainly due to the use of different tags, and also slightly different strains. The remaining differences might be due to the small variation in pH (7 versus 6.45). The chemical shift differences (CSPs) are shown in Fig. S3. Large CSPs between previous assignments and our sample were observed for residues K732, T737, A746, H752, K786 and I799. While the differences for the C-terminal I799 are likely due to the use of a different tag, the differences for the other residues remain unexplained. Most of the other CSPs remain below 0.2 ppm.

100



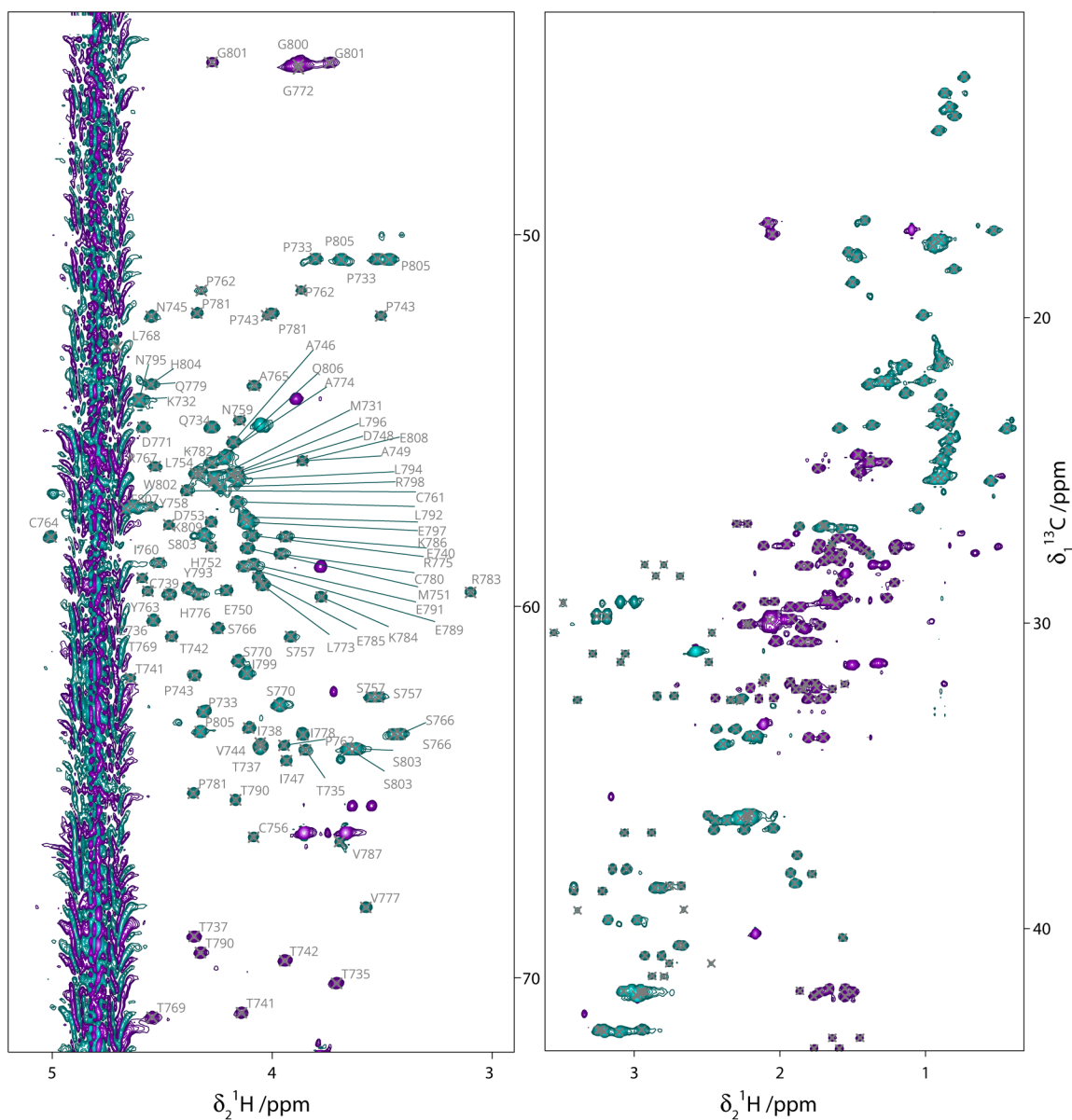


120 **Figure 3: NMRtist output graph, F1 score and percentage of assigned expected peaks in the different spectra.** (A) Extent and reliability  
of assignments obtained with the NMRtist automated resonance assignment algorithm using automatically picked peak lists. Each assignment  
for an atom is represented by a blue rectangle. Light colors indicate an assignment classified as weak by the chemical shift consolidation.  
(B) The box plots show the distribution of the F1 scores of the spectra, and the red dots represent the F1 scores calculated for the output of  
the peak picking application call. Scores above the median (dotted line) indicate that the automated peak picking routine was able to process  
a spectrum more accurately than 50% of the spectra in the benchmark. (C) Percentage of assigned peaks with respect to the expected number  
of cross peaks in each spectrum, as given by the protein sequence.

125



Peak assignments were manually verified using the Peak Predict module of the CCPN v3 software, and comparing the predicted peaks with the actual spectra, particularly the hCH spectrum. Some residues required small manual shifting, or completion of missing resonances.



130 **Figure 4:**  $^{13}\text{C}$  HSQC spectrum. (A)  $\text{C}\alpha/\text{H}\alpha$  region with assignments shown on the spectrum. (B) Side-chain region, with crosses indicating assigned peaks. For assignments see BMRB submission.

We identified several causes that led to (minor) problems in NMRtist assignments. Firstly, the fact that 3D backbone and side-chain spectra were not recorded on the same sample led to some inaccuracies, as spectra on deuterated protein were



used as is. While the  $^{15}\text{N}$ - HSQC were still very similar and many assignments could be transferred, slight differences led to  
135 increased errors. An additional error source was the relatively poor resolution of the HNcoCACB, which induced a greater  
uncertainty in the  $\text{C}\alpha$  and  $\text{C}\beta$  chemical shifts in this spectrum. Most problems were confined to regions where peak overlap  
occurred. Despite the few errors in the assignment, the use of NMRtist saved a lot of time, as all easy or isolated spin systems  
were quickly assigned with high confidence. It also turned out that for the relatively small protein used and the high spectral  
resolution, the backbone assignments did not help the program much, and the time needed for manual transfer of the  
140 assignments thereof could have been saved.

In the end, most of the side-chain carbon and proton assignments could be achieved, as shown in the extracts of the  $^{13}\text{C}$ -HSQC  
spectrum in Figure 4, where the assignments for the  $\text{H}\alpha/\text{C}\alpha$  are given, and all assigned side chains peaks are marked with a  
cross. The data have been deposited at the BMRB under accession number 52372.

#### 4. Discussion and Conclusion

145 We have shown here that the production and resonance assignment of small protein domains can be done in a highly efficient  
manner by combining cell-free protein synthesis, NMR spectroscopy on remote high-field platforms, and automated resonance  
assignment. The use of a high magnetic field not only provided the high resolution needed to assign side-chain protons, but  
also the sensitivity needed to study the below 150  $\mu\text{M}$  samples supplied by CFPS. While the sample preparation took about  
two days, the acquisition of the side-chain assignment spectra took 2-3 weeks, and the analysis 1-2 weeks to verify the  
150 automated assignments. The backbone assignments were not very time consuming since they had been previously established  
(Estrada and De Guzman, 2011), but required verification, which took several days when done manually, but was not necessary  
for automated assignments, which were similarly successful in the absence of this prior knowledge.

The protein considered here is rather small, with 69 amino acids plus a ten amino acid tag, and represents a subdomain of a  
larger, membrane-bound protein. While solid-state NMR can address the membrane-bound forms, solution-state NMR spectra  
155 of the isolated domains have the potential to accelerate a future analysis of the solid-state NMR 2D hCH and further 3D spectra,  
such as hCCH. The knowledge gained here will also be used to analyze the differences between the isolated and membrane-  
bound domain as highlighted by CSPs.

The number of situations where small domains can provide partial information on membrane-bound proteins is high in the  
study of viral proteins, as many viral envelope proteins carry rather small ecto- or cytosolic domains that are easily accessible  
160 to solution NMR. Together with AlphaFold2 predictions, sequential NMR resonance assignments can even obviate the need  
for structure calculations if the models are of high quality, since the secondary chemical shifts from sequential assignments  
provide immediate information on the secondary structure. The advantage of cell-free protein synthesis is that both membrane-  
bound and isolated domains can be produced with similar efficiency using the same approach.



### Author Contributions

- 165 LB analyzed backbone spectra and prepared, together with ML, figures; ML, together with CM, manually verified, and finalized the side-chain assignments; LC and MLF prepared samples; AB wrote the manuscript, with input from all authors; LL recorded the NMR spectra and ran the NMRtist analysis; MC analyzed the spectra and supervised the project together with MLF.

### Acknowledgements

- 170 Financial support from the IR INFRANALYTICS FR2054 for conducting the research is gratefully acknowledged.

### Data availability

Chemical shifts are submitted to the BMRB with the accession number 52372.

NMR spectra have been deposited to <https://doi.org/10.5281/zenodo.10938432>.

### Competing Interest

- 175 AB is Associate Editor with MR.

### References

- Arragain, B., Reguera, J., Desfosses, A., Gutsche, I., Schoehn, G., and Malet, H.: High resolution cryo-EM structure of the helical RNA-bound Hantaan virus nucleocapsid reveals its assembly mechanisms, *eLife*, 8, e43075, <https://doi.org/10.7554/eLife.43075>, 2019.
- 180 Arragain, B., Effantin, G., Gerlach, P., Reguera, J., Schoehn, G., Cusack, S., and Malet, H.: Pre-initiation and elongation structures of full-length La Crosse virus polymerase reveal functionally important conformational changes, *Nat Commun*, 11, 3590, <https://doi.org/10.1038/s41467-020-17349-4>, 2020.
- Arragain, B., Durieux Trouilleton, Q., Baudin, F., Provaznik, J., Azevedo, N., Cusack, S., Schoehn, G., and Malet, H.: 185 Structural snapshots of La Crosse virus polymerase reveal the mechanisms underlying Peribunyaviridae replication and transcription, *Nat Commun*, 13, 902, <https://doi.org/10.1038/s41467-022-28428-z>, 2022.
- Bignon, E. A., Albornoz, A., Guardado-Calvo, P., Rey, F. A., and Tischler, N. D.: Molecular organization and dynamics of the fusion protein Gc at the hantavirus surface, *eLife*, 8, e46028, <https://doi.org/10.7554/eLife.46028>, 2019.
- 190 Bonnet, S. I., Vourc'h, G., Raffetin, A., Falchi, A., Figoni, J., Fite, J., Hoch, T., Moutailler, S., and Quillery, E.: The control of Hyalomma ticks, vectors of the Crimean–Congo hemorrhagic fever virus: Where are we now and where are we going?, *PLoS Negl Trop Dis*, 16, e0010846, <https://doi.org/10.1371/journal.pntd.0010846>, 2022.
- Estrada, D. F. and De Guzman, R. N.: Structural Characterization of the Crimean-Congo Hemorrhagic Fever Virus Gn Tail Provides Insight into Virus Assembly, *Journal of Biological Chemistry*, 286, 21678–21686, <https://doi.org/10.1074/jbc.M110.216515>, 2011.
- 195 Estrada, D. F., Boudreaux, D. M., Zhong, D., St. Jeor, S. C., and De Guzman, R. N.: The Hantavirus Glycoprotein G1 Tail



- Contains Dual CCHC-type Classical Zinc Fingers, *Journal of Biological Chemistry*, 284, 8654–8660, <https://doi.org/10.1074/jbc.M808081200>, 2009.
- 200 Fogeron, M.-L., Badillo, A., Penin, F., and Böckmann, A.: Wheat Germ Cell-Free Overexpression for the Production of Membrane Proteins, in: *Membrane Protein Structure and Function Characterization*, vol. 1635, edited by: Lacapere, J.-J., Springer New York, New York, NY, 91–108, [https://doi.org/10.1007/978-1-4939-7151-0\\_5](https://doi.org/10.1007/978-1-4939-7151-0_5), 2017.
- Guardado-Calvo, P. and Rey, F. A.: The Envelope Proteins of the Bunyavirales, in: *Advances in Virus Research*, vol. 98, Elsevier, 83–118, <https://doi.org/10.1016/bs.aivir.2017.02.002>, 2017.
- 205 Halldorsson, S., Li, S., Li, M., Harlos, K., Bowden, T. A., and Huiskonen, J. T.: Shielding and activation of a viral membrane fusion protein, *Nat Commun*, 9, 349, <https://doi.org/10.1038/s41467-017-02789-2>, 2018.
- Hastie, K. M., Zandonatti, M. A., Kleinfelter, L. M., Heinrich, M. L., Rowland, M. M., Chandran, K., Branco, L. M., Robinson, J. E., Garry, R. F., and Saphire, E. O.: Structural basis for antibody-mediated neutralization of Lassa virus, *Science*, 356, 923–928, <https://doi.org/10.1126/science.aam7260>, 2017.
- Hawman, D. W. and Feldmann, H.: Crimean–Congo haemorrhagic fever virus, *Nat Rev Microbiol*, 1–15, <https://doi.org/10.1038/s41579-023-00871-9>, 2023.
- 210 Hulswit, R. J. G., Paesen, G. C., Bowden, T. A., and Shi, X.: Recent Advances in Bunyavirus Glycoprotein Research: Precursor Processing, Receptor Binding and Structure, *Viruses*, 13, 353, <https://doi.org/10.3390/v13020353>, 2021.
- Jirasko, V., Lends, A., Lakomek, N.-A., Fogeron, M.-L., Weber, M., Malär, A., Penzel, S., Bartenschlager, R., Meier, B. H., and Böckmann, A.: Dimer organization of membrane-associated NS5A of hepatitis C virus as determined by highly sensitive 1H-detected solid-state NMR., *Angewandte Chemie International Edition*, anie.202013296, <https://doi.org/10.1002/anie.202013296>, 2020.
- 215 Klukowski, P., Riek, R., and Güntert, P.: Rapid protein assignments and structures from raw NMR spectra with the deep learning technique ARTINA, *Nat Commun*, 13, 6151, <https://doi.org/10.1038/s41467-022-33879-5>, 2022.
- Lorenzo Juanes, H. M., Carbonell, C., Sendra, B. F., López-Bernus, A., Bahamonde, A., Orfao, A., Lista, C. V., Ledesma, M. S., Negredo, A. I., Rodríguez-Alonso, B., Bua, B. R., Sánchez-Seco, M. P., Muñoz Bellido, J. L., Muro, A., and Belhassen-García, M.: Crimean-Congo Hemorrhagic Fever, Spain, 2013–2021, *Emerg. Infect. Dis.*, 29, 252–259, <https://doi.org/10.3201/eid2902.220677>, 2023.
- 220 Matsuda, T., Kigawa, T., Koshiba, S., Inoue, M., Aoki, M., Yamasaki, K., Seki, M., Shinozaki, K., and Yokoyama, S.: Cell-free synthesis of zinc-binding proteins., *Journal of structural and functional genomics*, 7, 93–100, <https://doi.org/10.1007/s10969-006-9012-1>, 2006.
- 225 Mishra, A. K., Hellert, J., Freitas, N., Guardado-Calvo, P., Haouz, A., Fels, J. M., Maurer, D. P., Abelson, D. M., Bornholdt, Z. A., Walker, L. M., Chandran, K., Cosset, F.-L., McLellan, J. S., and Rey, F. A.: Structural basis of synergistic neutralization of Crimean-Congo hemorrhagic fever virus by human antibodies, *Science*, 375, 104–109, <https://doi.org/10.1126/science.abl6502>, 2022.
- 230 Strandin, T., Hepojoki, J., and Vaheri, A.: Cytoplasmic tails of bunyavirus Gn glycoproteins—Could they act as matrix protein surrogates?, *Virology*, 437, 73–80, <https://doi.org/10.1016/j.virol.2013.01.001>, 2013.
- Strecker, T., Eichler, R., Meulen, J. ter, Weissenhorn, W., Dieter Klenk, H., Garten, W., and Lenz, O.: Lassa Virus Z Protein Is a Matrix Protein Sufficient for the Release of Virus-Like Particles, *J Virol*, 77, 10700–10705, <https://doi.org/10.1128/JVI.77.19.10700-10705.2003>, 2003.
- 235 Sun, Y., Li, J., Gao, G. F., Tien, P., and Liu, W.: Bunyavirales ribonucleoproteins: the viral replication and transcription machinery, *Critical Reviews in Microbiology*, 44, 522–540, <https://doi.org/10.1080/1040841X.2018.1446901>, 2018.
- Takai, K., Sawasaki, T., and Endo, Y.: Practical cell-free protein synthesis system using purified wheat embryos, *Nature Protocols*, 5, 227–238, <https://doi.org/10.1038/nprot.2009.207>, 2010.
- Ye, W., Ye, C., Hu, Y., Dong, Y., Lei, Y., and Zhang, F.: The structure of Crimean-Congo hemorrhagic fever virus Gc is revealed; many more still need an answer, *Virologica Sinica*, 37, 634–636, <https://doi.org/10.1016/j.virs.2022.05.003>, 2022.
- 240 Zhu, Y., Wu, Y., Chai, Y., Qi, J., Peng, R., Feng, W.-H., and Gao, G. F.: The Postfusion Structure of the Heartland Virus Gc Glycoprotein Supports Taxonomic Separation of the Bunyaviral Families Phenuiviridae and Hantaviridae, *Journal of Virology*, 92, e01558-17, <https://doi.org/10.1128/JVI.01558-17>, 2017.